JOURNAL OF CATALYSIS 59, 153–167 (1979)

Hydrogenation of Olefins and Polymerization of Ethene over Chromium Oxide/Silica Catalysts

I. Preparation and Structure of the Catalyst

C. GROENEVELD,[1] P. P. M. M. WITTGEN,[2] A. M. VAN KERSBERGEN, P. L. M. MESTROM, C. E. NUIJTEN, AND G. C. A. SCHUIT

Department of Inorganic Chemistry and Catalysis, Eindhoven University of Technology, The Netherlands

Received May 12, 1977; revised September 11, 1978

The structure, texture, degree of dispersion, and valency of Cr were investigated for CrO_x/SiO_2 catalysts as a function of the method of impregnation, calcination, and subsequent reduction. The catalysts were characterized by analytical methods, by uv-visible spectroscopy, and by EPR and paramagnetic susceptibility measurements. Impregnation with or adsorption from CrO_3 solutions leads in the first instance to binuclear chromate complexes adsorbed on the silica surface. Reduction with H_2 or C_2H_4 results in catalysts containing both Cr^{2+} and Cr^{3+} ions, the latter in various states of clustering. In agreement with the literature it was found that the removal of produced water was crucial, higher efficiencies in water removal leading to higher Cr^{2+}/Cr^{3+} ratios and less tendency to Cr^{3+} clustering. Surprisingly, reoxidation of Cr^{2+} occurred also when the catalyst was reduced with CO. This reoxidation was found to be caused by silanol groups.

INTRODUCTION

Catalysts based on chromium oxide for polymerization [Phillips process (*1*)], (de)-hydrogenation [Houdry process (*2*)], and dehydrocyclization of hydrocarbons have been of industrial interest for many years and consequently the subject of many investigations. So far, however, the understanding of the reaction mechanism and the active sites (their valence state and coordination) remains incomplete and the theoretical models proposed are often contradictory.

The present paper is the first of a series which deals with the polymerization of ethylene and the hydrogenation of olefins over chromium oxide/silica catalysts. In this paper we shall try to elucidate the structure of the catalyst common to both processes. The following papers will be concerned with the mechanism of the polymerization and with that of the hydrogenation. To become active the catalyst has to be reduced. The reduction was carried out with H_2 or CO. Although technically more common the reduction with ethylene and/or solvent will not be discussed here, since it is rather complex and does not present essential new information about the structure of the final catalyst.

[1] Present address: Central Laboratory, Dutch States Mines, P.O. Box 18, Geleen, The Netherlands. To whom correspondence should be addressed.

[2] Present address: Chemical Laboratory, TNO, Lange Kleiweg 137, P.O. Box 45, Rijswijk (ZH), The Netherlands.

0021-9517/79/110153-15$02.00/0

EXPERIMENTAL

Catalyst Preparation

A silica carrier (usually Davison silica gel, grade 12; specific surface area 600 m^2/g; pore volume 0.4 cm^3/g; less frequently Degussa aerosil, specific surface area 200 m^2/g) was impregnated with a solution of chromium trioxide (Merck, p.a.) in water. With respect to the method of impregnation we distinguish two types of catalyst.

Type I. The carrier is impregnated with an amount of solution which is not quite sufficient to make the particles stick together. This amount should be equal to the pore volume. Sometimes aerosil was used here.

Type II. The carrier is suspended in a relatively large amount of chromic acid solution and the suspension is stirred and filtered after a few hours. During this procedure the temperature does not exceed 30°C.

Both types of catalyst were dried for 16 hr at 105°C and divided into two sieve fractions ($0.09 < d < 0.175$ mm and $0.175 < d < 0.60$ mm). Afterwards the catalyst was calcined in air at 500°C for 4 hr and stored over P_2O_5 because of its hygroscopic properties.

The chromium content of the dry catalyst was determined iodometrically or spectrophotometrically according to standard prescriptions (*3*), after removing the silica as SiF_4 by treating the catalyst with HF. The specific surface areas of the catalysts and the carriers were measured according to the BET method with nitrogen at −196°C.

When not specified the chromium content was 2 wt% (1.83–2.07 wt%) and the carrier Davison silica gel.

Reduction with CO

Pulses of carbon monoxide (1.39 cm^3) were injected into a stream of helium (75 cm^3/min). After passing the quartz reactor the pulses were analyzed by glc in combination with a heat conductivity cell. In all experiments a fixed bed of 1 g of catalyst was used and the interval time between successive pulses was 8 min.

Reduction with H_2

Pulses of hydrogen (0.273 cm^3) were injected into a stream of argon (50 or 100 cm^3/min). The amount of hydrogen which passed the reactor was detected with the help of heat conductivity cell. A fixed bed of 0.5 or 5 g of catalyst was used.

Thermal Analysis (DTA/TGA)

Using the Dupont apparatus it was possible to heat (rate: 5 or 10°C/min, range: up to 500°C) the sample (18 mg) in a gas stream with a space velocity of 750 cm^3/min.

Magnetic Susceptibility

The measurements were performed according to the Gouy method at temperatures between −180 and 100°C. After correcting for the diamagnetism of the silica and the sample holder, the effective magnetic moment P_{eff} and Weiss constant θ were obtained from a plot of the magnetic susceptibility vs the reciprocal temperature.

Assuming spin-only magnetism the number of unpaired electrons per chromium atom (n) is given by

$$P_{\text{eff}} = [n(n+2)]^{\frac{1}{2}}. \qquad (1)$$

According to Heisenberg θ can be written as

$$\theta = \frac{-2JZS(S+1)}{3k} \qquad (2)$$

where J is the exchange integral, Z the number of paramagnetic neighbor ions, S the spin quantum number, and k the Boltzmann constant. For ferromagnetic coupling the sign of J is negative and therefore θ is positive, while for antiferromagnetic coupling J and θ are positive and negative, respectively.

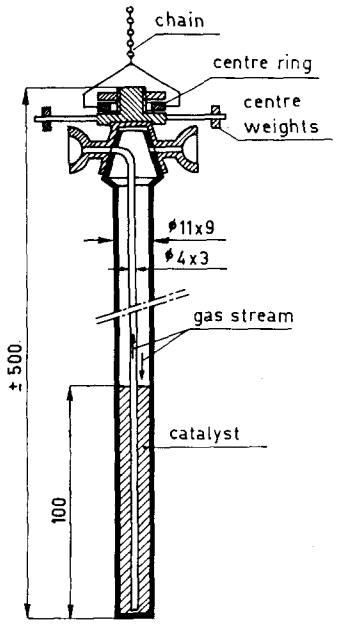

FIG. 1. Glass sample holder for magnetic susceptibility measurements.

The sample holder (Fig. 1) was constructed in such a way that the catalyst could be treated in various ways and then be transported to the Gouy balance under exclusion of air.

Electron Paramagnetic Resonance

Two types of measurement were performed.

(a) The sample was treated *in situ* in a Varian spectrometer (type E 15) equipped with a high-temperature cavity (*4*). This was done in a special sample holder (Fig. 2a). By using a reference signal (Varian strong pitch No. 904456-01; $3.10^{15} \pm 25\%$ spins/cm) it was possible to determine the g value of the various signals and to estimate the amounts of ions corresponding to these signals.

(b)The sample was treated outside the spectrometer. The sample holder (Fig. 2b) was constructed in such a way that the catalyst could be brought into an A.E.G. spectrometer under exclusion of air. The conditions of catalyst treatment were better defined in this case.

In all cases the first derivative of the absorption curve was recorded. The microwave frequency was about 10 GHz. Three signals were reported so far for chromium oxide-on-carrier samples, commonly called β, γ, and δ signals. The β signal is at $g = 1.9$ to 2.8; it is broad (width about 80–180 kA/m) and is attributed to clusters of Cr^{3+} ions which are antiferromagnetically coupled. The γ signal is at $g = 1.90$ to 2.00; it is small (width about 1 kA/m) and is assigned to Cr^{5+} ions in a tetragonal pyramidal coordination. The δ signal is at $g = 3.5$ to 4.5; its width is about 40 kA/m and it is believed to be connected with isolated Cr^{3+} ions in a distorted octahedron (*5*, *6*).

Reflectance Spectroscopy

Reflectance was measured according to the diffuse reflectance method with a Uni-

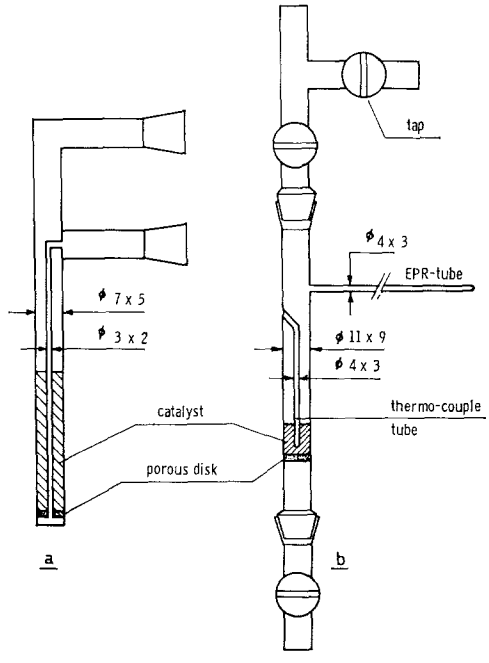

FIG. 2. Quartz glass sample holder for EPR measurements: (a) sample holder used with Varian high-temperature cavity; (b) sample holder used with the AEG cavity.

cam spectrometer (type SP 800). The sample holder (Fig. 3) enabled the catalyst to be treated in various ways and then be transported to the spectrometer under exclusion of air. The catalyst was powdered for this purpose and then pressed (290 MPa) into a thin disk. The sample was heated with a spot heater. Only CO-reduced catalysts were examined.

Infrared Spectroscopy

Spectra of the catalyst were obtained by pressing thin disks (100 mg, surface area 6.16 cm^2, thickness 0.1 mm) at 290 MPa and pretreating and studying these *in situ*. Only a few results will be dealt with here; a more extensive description of the ir studies and a description of the ir cell will be given in a later paper (*7*).

Gas Purification

All gases were freed from traces of oxygen (except in the cases of oxygen or air) by a BASF copper catalyst and from moisture by molecular sieves. If necessary carbon dioxide was removed by cooling the molecular sieves. Hydrogen was usually purified by diffusion through a palladium membrane. After the investigation it became apparent that a BASF copper catalyst may not have been sufficient to handle Cr^{2+} on silica gel completely oxygen free (*8*). However the residual amounts of oxygen in the carrier gas are too small to explain the experimental phenomena described in this article.

TABLE 1

UV-Visible Reflectance Spectra

Sample	Absorption bands (cm^{-1})[a]
Calcined catalyst[b]	20,500 (s); 28,800 (s); 38,200 (s); 47,000 (s); 51,000 (w)
Catalyst reduced with CO, 440°C[b]	14,500 (m); 20,700 (w)
Catalyst after reoxidation, 320°C[b]	14,500 (vw); 20,700 (m)
Silica gel	38,000 (w); 47,200 (s); 51,500 (w)
$K_2Cr_2O_7$	20,400 (s); 25,000 (w); 25,900 (w); 26,700 (w); 29,800 (s); 38,500 (s); 44,000 (m); 51,000 (m)
K_2CrO_4	23,100 (s); 25,800 (w); 29,700 (s); 34,200 (m); 38,000 (m); 43,000 (m)

[a] s, strong; m, medium; w, weak; vw, very weak.
[b] Catalyst contained 1.7 wt% Cr.

RESULTS

Catalyst after Calcination

After calcination the color of the catalyst is yellow–orange. Reflectance spectra (Table 1) show a strong absorption band

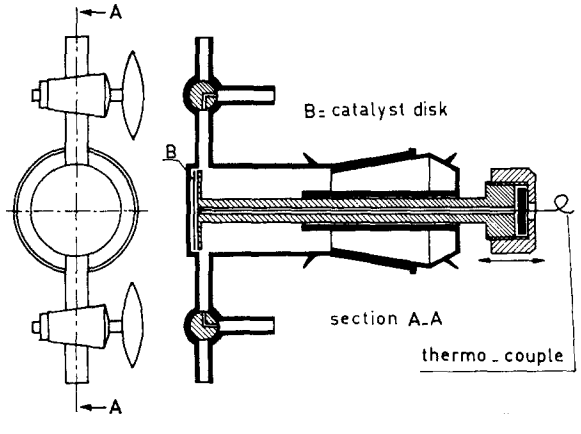

FIG. 3. Glass cell for *in situ* reflectance spectroscopy.

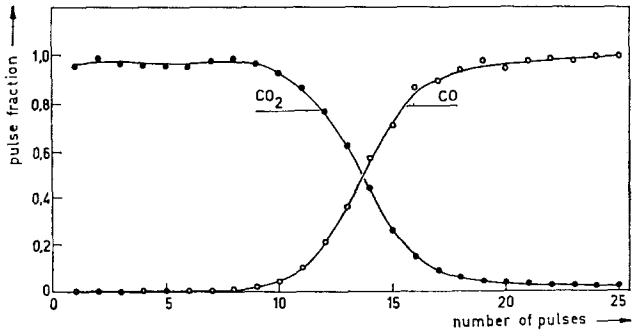

FIG. 4. CO and CO_2 detected in the course of the reduction of 1 g catalyst (II) with CO pulses (1.39 cm^3) at 470°C.

at 20,500 cm^{-1} which corresponds well with the absorption band at 20,400 cm^{-1} of potassium bichromate. Since the acidity of the chromic acid solution used in the preparation is so high that the chromium ions are present as bi- or polychromates (*9*), it is to be expected that the chromium ions are not present on the silica surface as isolated species but coupled as in potassium bichromate. Normally chromic acid decomposes above 255°C but the yellow–orange color persists at temperatures up to 500°C so the silica surface appears to stabilize chromic acid.

Most investigators (*10–12*) explain this effect by assuming a condensation reaction of chromic acid with hydroxyl groups of the silica surface (≡ stabilization). Such a reaction would explain the exothermal effect found in DTA measurements between 250 and 350°C.

Magnetic susceptibility measurements indicate an average valence state of chromium near six (>5.9). Electron paramagnetic resonance spectra show a weak broad δ signal (ΔH = 40 kA/m) at g = 4.6, a broad β signal (ΔH = 80 kA/m) at g = 2.4 to 2.8, and a narrow $2g$ value γ signal (ΔH = 1 kA/m) at g_{av} = 1.96 ($g_{\perp}$ = 1.97, $g_{\parallel}$ = 1.95).

For reasons which will become apparent this γ signal will be called γ_1. The concentration of chromium (III) and chromium (V) measured with EPR amounted to 0.15 and 0.7% of the chromium present.

Reduction with CO

The first 10 pulses of carbon monoxide are fully oxidized (Fig. 4). Hereafter the amount of CO_2 produced per pulse becomes less and finally very small, although still observable. The color of the catalyst (type II) changed on reduction from orange to blue–green and on prolonged treatment with CO to blue. In the reflectance spectra (Table 1) an absorption band appears at 14,500 cm^{-1}, which can be ascribed to Cr^{3+} (*13*) or Cr^{2+} (*14*). However, with Cr^{3+} one would also expect the presence of a band at 23,000 cm^{-1} (*13*) and, since this is not observed, the band at 14,500 cm^{-1} is ascribed to Cr^{2+} in a square planar coordination. When a catalyst so reduced was oxidized again at 470°C, no CO_2 was detected and also carbon-mass balances of the CO pulses did not reveal the presence of residual carbon on the CO-reduced catalyst.

With EPR we found that the δ signal [isolated Cr^{3+} in distorted octahedron (*15*)] shifted on reduction from g = 4.6 to 3.6. According to van Reijen (*15*) this shift must be due to a changed symmetry of the octahedron. At the same time its intensity increased; however, the amount of ions that corresponds with the signal constituted about 0.1% of the total amount of chromium present.

The intensity of the γ_1 signal (Cr^{5+} in square pyramidal coordination) decreased

rapidly during the reduction; another small signal (which we will call γ_2) became observable and its intensity increased. On prolonged reduction, however, this signal also disappeared completely. The γ_2 signal (with $g_\perp = 1.98$ and $g_\parallel = 1.91$) could be due to Cr^{5+} in a surrounding with a lower symmetry (adsorbed water) to that corresponding to the γ_1 signal (*16–18*), but also to Cr^{4+} in a tetrahedral coordination.

Whatever the situation may be, the amount of ions corresponding to the γ signals is very small during the whole reduction ($\ll 0.1\%$). The intensity of the β signal increased at first during the CO treatment (max about 2% of the total amount of Cr ions), but on prolonged reduction it decreased to an intensity that corresponded with about 1.6% of all the chromium present. It was also interesting that the intensity of the β signal increased with temperature, whereas it should decrease according to the Curie law. This effect must be due to the existence of an antiferromagnetic coupling between the Cr^{3+} ions. The g value of the β signal is 2.25 and since this is in between the g value of isolated Cr^{3+} ions (3.6) and that of Cr^{3+} in Cr_2O_3 (1.98), Carman and Kroenke (*19*) ascribe it to Cr^{3+} in less complete coupling than in Cr_2O_3.

Calculating the average valency of the chromium from the amounts of CO_2 produced and assuming all CO_2 to be produced by reduction of chromium, we find (Fig. 5) that the average calculated valency drops rapidly to about 2.5. Prolonged CO treatment, corresponding to the right part of Fig. 4, lowers the calculated valency to even below 2.0. Since an average valency below 2.0 would imply the presence of Cr^+ or Cr^0 and since we obtained an average valency of 2.5 from magnetic susceptibility data (Table 3), we were interested in the origin of the small CO_2 production as CO is passed over a reduced catalyst. A revealing detail in this context is that on varying the interval time t between the pulses the amount of CO_2 produced increases linearly with $t^{\frac{1}{2}}$ (Fig. 6).

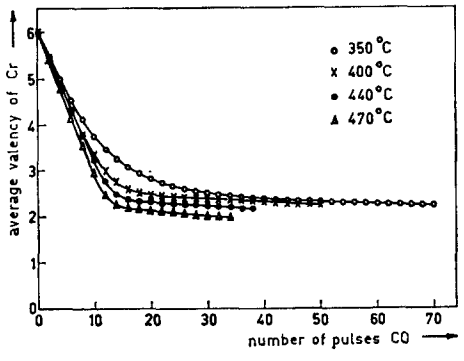

FIG. 5. Average valency of chromium calculated from the amounts of CO_2 produced in the course of the reduction with CO.

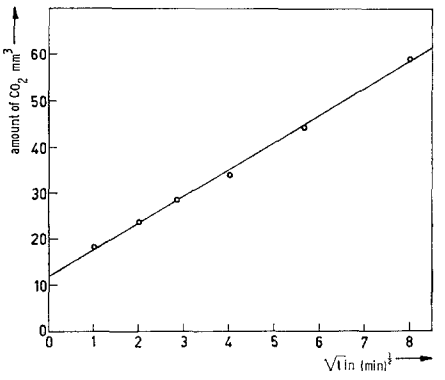

FIG. 6. Amount of CO_2 produced as a function of the square root of the pulse interval time. Temperature: 440°C; CO-reduced catalyst.

The CO_2 production can be caused by different reactions, which we shall divide into four categories.

(a) True reduction to Cr^+ or Cr^0. Not only does this disagree with the magnetic susceptibility data, but such reactions also appear to be thermodynamically highly unfavorable (*20*).

(b) Carbide formation according to Eq. (3). This thermodynamically easy reaction can be ruled out because no carbon residue could be detected on the catalyst.

$$3Cr_2O_3 + 17CO \rightarrow 2Cr_3C_2 + 13CO_2 \quad (3)$$

(c) Boudouard reaction according to

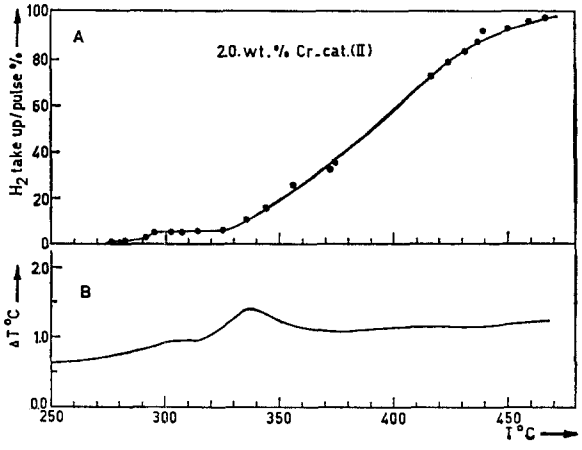

FIG. 7. (A) Rate of reduction expressed by the H_2 take-up per pulse H_2 (0.273 cm^3) per 5 g catalyst (II). (B) DTA recording during the reduction.

Eq. (4). Also in this case the presence of carbon should have been detected. Furthermore this explanation does not agree with the above-mentioned $t^{\frac{1}{2}}$ dependence of the CO_2 production.

$$2CO \rightarrow C + CO_2 \qquad (4)$$

(d) Chromium is oxidized by some oxidizing agent in the intervals between pulses, so that the reduction can start again. This explanation is in our opinion the correct one, and implies that the valency calculated from the amounts of CO_2 produced is not the real valency. In the discussion we shall go into this in more detail. However, it is important to point out that the oxidizing agent cannot have been oxygen (from leakage or helium impurity), because of the above-mentioned $t^{\frac{1}{2}}$ dependence of the CO_2 production. Also the amount of oxygen normally present in the helium carrier gas (1 ppm) would have been quite insufficient to produce the amounts of carbon dioxide detected.

One final observation that is of interest is that 1 g of CO-reduced catalyst appeared to be able to adsorb about 9 cm^3 CO and about 6 cm^3 O_2 at 0°C and 1 atm. This means average ratios CO/Cr of 0.97 and O/Cr of 1.34 based on total chromium present.

After O_2 adsorption the color of the catalyst was dark brown, but on further exposure to air it changed to yellow–brown. The chromium ions therefore appear easily accessible to molecules from the gas phase, i.e., they are present at the surface.

Reduction with Hydrogen

The rate of reduction of the catalyst (II) was measured in the pulse apparatus as a function of the reduction temperature by observing the fractional decrease per pulse at different temperatures. Below 330°C the rate of reduction is low. Above 330°C Fig. 7a shows a steady increase of the rate. Information about the realizable reduction levels of the catalyst (II; exceptionally 1.4 wt% Cr) is given in Fig. 8. The average calculated valency of chromium is 3.9, 2.9, and 2.2 at 350, 410, and 450°C, respectively.

Hereafter, repeated calcination and reduction of the catalyst (referred to in the literature as cycling or stabilization of the catalyst) has only a small influence on the average valency. Especially after reduction the average valency was not much lower.

Differential thermal analysis (Fig. 7b) of the reduction of the catalyst in hydrogen atmosphere indicates an overall exothermic

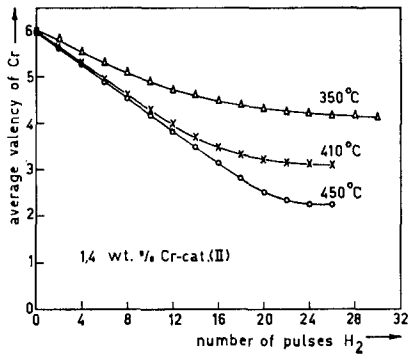

FIG. 8. Average valency of chromium calculated from the H_2 take-up in the course of the reduction with H_2.

effect (20–450°C) with an extra exothermic effect in the range 300 to 370°C with a maximum at 340°C superimposed on it. This maximum is near the temperature whereby the reduction rate suddenly increases. In none of the samples was the "glow phenomenon," first noticed by Berzelius, observed. The weight of the sample decreases gradually by 1%. In this stage of the investigation catalysts reduced with hydrogen were colored green.

On carrying out EPR measurements whereby the reduction was followed *in situ*, we discovered that the degree of reduction of the catalyst depends on factors such as rate of heating and the linear gas velocity through the catalyst bed. If the rate of heating is low (< 15°C/min; $T_{red} = 500$°C) and the linear gas velocity of hydrogen is more than 400 cm/min the catalyst became blue. A green colored sample was obtained when the rate of heating was high (> 50° C/min; $T_{red} = 500$°C) and the linear gas velocity of hydrogen was low. EPR spectra of the reduction of the catalyst *in situ* by the first procedure are presented in Figs. 9a and b (detail). The spectrum at 150°C

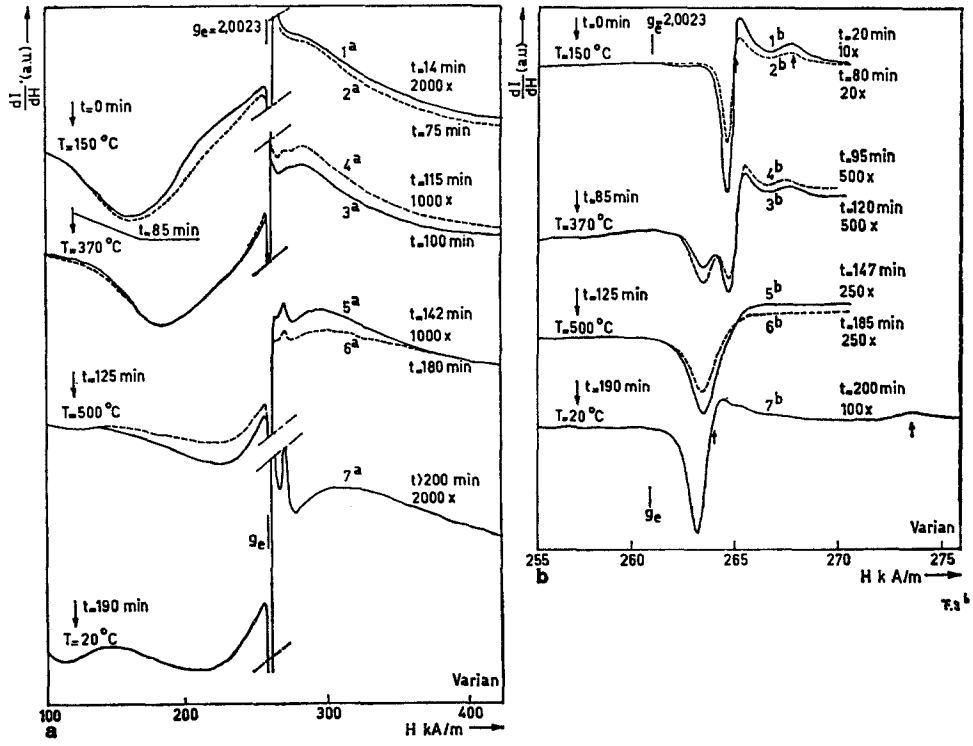

FIG. 9. EPR spectra of catalyst (II) in various stages of reduction with H_2 (time at the left: moment of temperature increase; time at the right: moment of recording). (a) spectra between 100 and 400 kA/m; (b) detail spectra of (a).

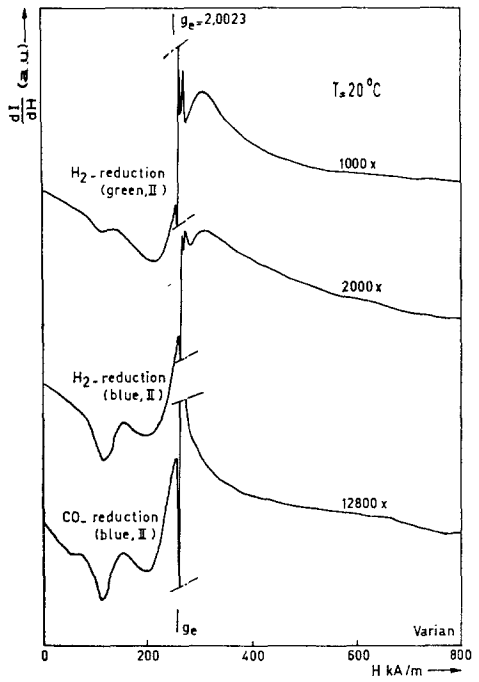

FIG. 10. EPR spectra of catalysts (II) after reduction with H_2 (green: < 40 cm³ H_2/min; blue: > 100 cm³ H_2/min) and reduction with CO.

shows the broad (ΔH = 111kA/m) β signal ($g \simeq 2.4$) and the γ_1 signal which had been noticed already during the reduction with CO. Considering the inflection point the β signal must be made up of two signals. One of these, henceforth called β_2, has an average g value of 2.4 that however can vary from 2.4 to 2.8 for different samples. It corresponds to Cr^{3+} in magnetically less complete coupling than in Cr_2O_3. The other (β_1) with a g value of 1.98, corresponds to the β signal in the literature, as will be shown later. The combined signal moves to a lower g value in the course of the reduction, presumably because of an increase in the intensity of the β_1 signal and a shift to lower g value (more magnetic coupling) of the decreasing β_2 signal.

In the course of the reduction the detailed spectrum shows a rise of the γ_2 signal beside a gradual decrease in intensity of the γ_1 signal. Both γ signals disappeared completely when the reductions were carried out under optimal conditions. The δ signal is just observed at 500°C. On cooling the sample to room temperature the δ signal increases while the remaining β_1 signal decreases, presumably because of increasing antiferromagnetic coupling. The concentrations of chromium in the β, δ, and γ_2 phases detected at room temperature amount to 24, 0.8, and 0.4%, respectively.

For comparison the EPR spectra and the concentrations of the different chromium ions in samples reduced in hydrogen (green and blue samples) and in a sample reduced in CO are presented in Fig. 10 and Table 2, respectively. A better defined reduction was realized when the reduction with hydrogen was carried out outside the spectrometer in the special reactor. Figure 11 represents spectra of different catalysts

TABLE 2

EPR g Values and Chromium Concentrations[a]

	β Cr^{3+}		δ Cr^{3+}		γ_2 Cr^{5+}			γ_1 Cr^{5+}		
	g	% Cr	g	% Cr	$g_\perp$	$g_\parallel$	% Cr	$g_\perp$	$g_\parallel$	% Cr
H_2 reduction green catalyst	1.98	26	3.6	0.3	1.98	1.90	0.4	1.97	1.95	—
H_2 reduction blue catalyst	1.98	24	to	0.8	1.98	1.90	0.4	1.97	1.95	—
CO reduction blue catalyst	2.19	1.5	3.8	0.13	1.98	1.90	<0.01	1.97	1.95	—

[a] Calculated from spectra in Fig. 10 (γ_2 signal calculated as Cr^{5+}).

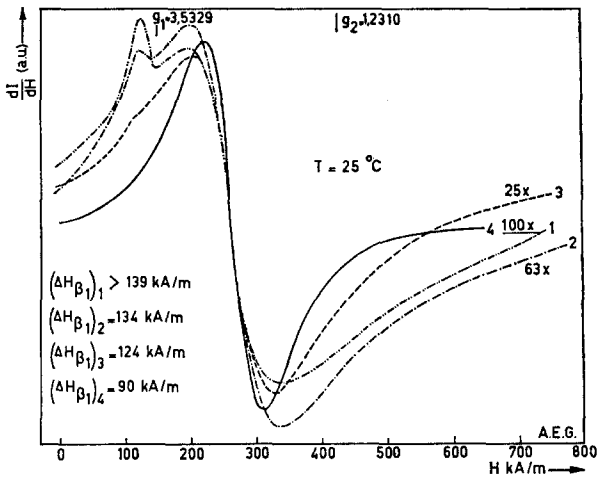

FIG. 11. EPR spectra of amorphous chromia and catalysts after reduction with H_2 at 495°C: (1) catalyst (II; H_2: blue); (2) catalyst (II; H_2: green); (3) catalyst (I; H_2: green); (4) amorphous chromia (treated in H_2 at 300°C).

thus prepared, viz.: (1) catalyst (II; H_2: blue), (2) catalyst (II; H_2: green), (3) catalyst (I; H_2: green), and (4) amorphous chromia (H_2: green). No γ phase is present in the samples.

The average chromium valency of catalyst (II; H_2: green) turns out to be 3.0. Also here only a small effect of "cycling" of the catalyst was observed on the average valency of chromium. The valency decreased after the second calcination–reduction cycle to 2.9. Hereafter repeated cycling did not have any effect. The Weiss constant ($|\theta|$) ranged at random between 140 and 205°K.

Because of the dimensions of the sample holder for magnetic measurements it was impossible to obtain a blue catalyst by hydrogen reduction in that sample holder. However, since the average valency in CO-reduced catalyst (II; CO: blue) is 2.5 and EPR spectra showed that catalyst (II; H_2: green) is less reduced than catalyst (II; H_2: blue) we may assume an average valency of the latter between 2.5 and 3.0.

For comparison, the results of the magnetic susceptibility measurements and the valency calculated from H_2 consumption or CO_2 production are presented in Table 3.

Surface Area and X-Ray Diffraction

None of the samples reduced in CO or H_2 showed any crystallinity. The surface area (Davison) was about 500 m^2/g and did not change appreciably after the various treatments.

Infrared Spectroscopy

IR spectra of CO- or H_2-reduced catalysts always show bands at 1000 to 1250 cm^{-1} (Si–O stretching and SiOH bending), 1600 to 1700 and 1800 to 1900 cm^{-1} (overtones and combination vibrations of SiO bands), and a strong band at 3400 to 3700 cm^{-1} (OH stretching), the assignments being derived

TABLE 3

Chromium Valency for Different Catalyst Samples Calculated by Different Methods

	Valency from magnetic susceptibility	Valency from CO_2 production/H_2 consumption
Catalyst (II; CO: blue) T_{red} = 470°C	2.5	<1.9
Catalyst (II; H_2: green) T_{red} = 470°C	3.1	2.3 (T_{red} = 450°C)

from Benesi and Jones (*21*). The O–H stretchings always remain observable although evacuating (1.3 mPa, 450°C) tends to diminish their intensity.

If a CO-reduced catalyst is subsequently treated with D_2 at 200°C a broad absorption band develops at 2550–2760 cm^{-1} which is undoubtedly due to O–D stretchings.

DISCUSSION

The final state of the catalyst depends on the various stages of catalyst preparation. For example, not only is the reduction gas important but also other factors such as hydrogen gas velocity and heating rate during the reduction. The water gas equilibrium [Eq. (5)] shows that hydrogen is a slightly less powerful reducing agent than CO.

$$H_2O + CO \rightleftarrows H_2 + CO_2$$
$$\Delta G_T^0 = -30 + 0.042\,(T\text{-}298)\ \text{kJ/mole}. \quad (5)$$

To what extent the degree of reduction will be different after CO or H_2 treatment will depend on the remaining factors, which point to the well-known influence of water (*22*, *23*).

Confining ourselves first to catalyst (II), three types can be distinguished after reduction, as indicated by the EPR spectra (Fig. 10). From these three types the two blue-colored catalysts (especially the catalyst after CO reduction) turn out to be further reduced than the green one. Their blue color (absorption band at 14,500 cm^{-1} and no absorption at 23,000 cm^{-1}) points to the presence of chromium (II) ions in appreciable quantities.

The EPR spectrum of catalyst (II; CO: blue) shows only a very small β signal compared with the catalysts (II; H_2: blue) and (II; H_2: green). The δ signal of both blue catalysts is relatively large compared with their β signal. This points to the presence of more isolated chromium in the blue catalyst than in the green one. The effect is even more clear if the spectra in Fig. 11 are compared with each other. The δ signal of catalyst (I; H_2: green) is very small and we may assume in view of the impregnation method used that the chromium ions are poorly distributed over the surface (in amorphous chromia a δ signal cannot be detected). In contrast with the intensity the peak width (ΔH) of the β_1 signal decreases in the order: catalyst (II; H_2: blue) > catalyst (II; H_2: green) > catalyst (I; H_2: green) > pure chromia. A smaller peak width indicates a larger exchange interaction, so the total antiferromagnetic interaction between the chromium (III) ions is becoming larger as a consequence of a worse distribution of the chromium ions over the surface. The more the latter is the case the more the spectra resemble that of amorphous chromia.

Magnetic susceptibility data are in agreement with the EPR results. The Weiss constant (θ) for the green catalyst is larger than for the blue ones. For the green catalyst θ is maximally 200 K. For α-Cr_2O_3 θ is 485 K (*24*) and since in both cases J as well as S will be the same (*25*) it follows that in the green catalyst the average number of paramagnetic neighbor ions will be about 3. Once the catalyst is green, it proves to be very stable to reduction. Apparently the chromium (III) ions are stabilized by a strong crystal field, which is characteristic for α-Cr_2O_3. This implies that the chromium oxide particles on the surface are three dimensional. However, no Néel point [α-Cr_2O_3: T_N = 34°C (24)] could be detected and the magnetic susceptibility obeyed the Curie–Weiss law. Therefore we conclude, following Srivastava (*26*), that these particles have to be smaller than 5 nm.

The Weiss constant for the blue catalyst ranges from 120 to 160 K. Taking into account that in this case S is larger than in the case of the green catalyst, it is now found that the number of paramagnetic neighbor ions will be about 2. Since the

magnetic susceptibility data indicate that a large amount of chromium (II) is present (Table 3), no stabilization of chromium (III) has occurred and the chromium oxide has to be present as flat or extremely small spherical particles. The CO adsorption on catalyst (II; CO: blue) supports the model of flat particles. Each chromium ion seems to be capable of adsorbing one gas molecule (CO/Cr = 0.97) at least when we assume the formation of Cr–CO complexes with the stoichiometry 1:1. For our conditions of calcination and reduction (respectively at 500 and 470°C) Krauss *et al.* (*27*) have proven that at least for Cr^{2+} this is indeed the case.

So far the differences in the catalysts originate partially from different reduction agents or different impregnation methods. However, the differences between catalyst (II; H_2: blue) and catalyst (II; H_2: green) can be explained only when kinetic factors such as gas velocity and heating rate during the reduction are taken into account. Combined with the fact that there are differences in crystal field stabilization after the reduction with CO or H_2, this indicates again that water produced during the reduction has a large influence on the catalyst (*22*, *23*). A high heating rate causes a large water production, which cannot be removed fast enough by the gas stream.

What are the reactions that take place at the surface during the preparation of the catalyst and the ensuing reduction? Because of the high acidity of the chromic acid and the low temperature used during the impregnation of silica with chromic acid the initial formation of bi- or polychromates at the surface seems indicated (*9*).

The presence of bichromate is indeed confirmed by reflectance spectra measurements. It should be realized that even if the chromic acid is adsorbed as a "monolayer," it will not cover more than 5% of the surface area. During the calcination the chromic acid becomes stabilized by interaction with the silica surface [Eq. (6)] (*10–12*). This was shown not only by the DTA measurements but also by the absence of a decomposition into α-Cr_2O_3.

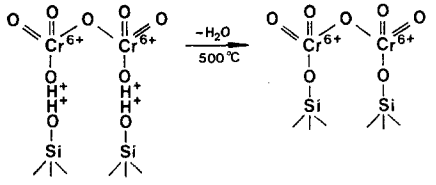

(6)

The reduction of the catalyst with H_2 or CO can be represented by Eq. (7).

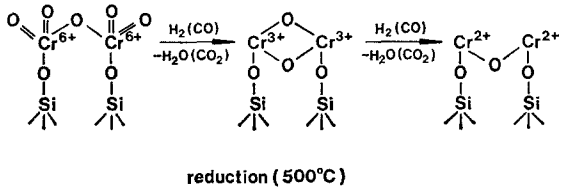

(7)

In contrast with CO_2 water produced during the reduction can influence the reduction. If it is not removed fast, it adsorbs at the silica surface. At high temperatures (>300°C) the adsorbed water becomes mobile and chemically more active.

Then it can act in two ways: (i) it oxidizes chromium (II) to chromium (III); (ii) it hydrolyzes the Si–O–Cr bonding.

Case 1

Water oxidizes chromium (II) to chromium (III) [reverse of second step in

Eq. (7)]. Already at a low relative water vapor pressure ($P_{H_2O}/P_{H_2} > 8 \times 10^{-6}$) chromium (II) oxide is not stable thermodynamically. This effect of water influences the degree of reduction directly. In addition to the water produced during the reduction with H_2, there is already water present at the silica surface in the form of hydroxyl groups. These groups become active at high temperature. We assume this to be the explanation for the discrepancy between the average valency of chromium calculated from the magnetic susceptibility and from the pulse method. In the section dealing with the reduction with CO we put forward the idea of an oxidizing agent which oxidizes chromium (II) to chromium (III) that can subsequently be reduced again by CO. This process was found to be linearly related with the square root of the time. For this the transport of the hydroxyl groups over the silica surface followed by an oxidation as just described is a ready explanation. From measurements at different temperatures it was found that this transport process, which is actually a proton jump between lattice oxygen ions, would have an activation energy of 50 kJ/mole. This agrees very well with the values of 20 to 42 kJ/mole found by Freude *et al.* (*28*) for the proton jump in zeolites. The interaction of the hydroxyl groups at the silica surface with the chromium oxide phase has been confirmed by the ir reflection measurements and also by H_2/D_2 exchange and H_2 adsorption measurements which will be reported later (*29, 30*) and which showed that the adsorption of hydrogen and deuterium goes via the chromium oxide phase followed by a spill-over effect to the silica surface. Similar effects were noticed by Schuit and de Boer (*31*) in the system Ni/SiO_2. A prolonged reduction with intermediate reoxidation by hydroxyl groups will therefore cause a gradual dehydration of the silica surface with only a very slowly declining average valency. This is affirmed by the fact that the color changes from blue–green (mixture Cr^{3+}, Cr^{2+}) to blue (Cr^{2+}) during extensive reduction. It should be stressed here that this picture plays an important role in our model of the active polymerization site (*7, 32*). Thus calculating the average valency from the CO_2 production (reduction with CO) or the H_2 consumption (reduction with H_2) results in values that are too low because of reoxidation between pulses.

Case 2

Water hydrolyzes the Si–O–Cr bonding after which the chromium oxide regains its mobility across the surface. This results in the formation of bigger conglomerates [Eq. (8)] that are less stabilized or not at all stabilized by the surface, and therefore reduced to Cr_2O_3.

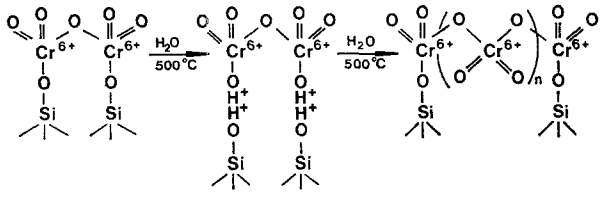

(8)

Because of the strong crystal field stabilization, Cr_2O_3 is rather stable with regard to oxidation or reduction. This clustering might be the explanation for the shift of the β_2 EPR signal from $g = 2.4$ to 1.98 (corresponding with the β phase in

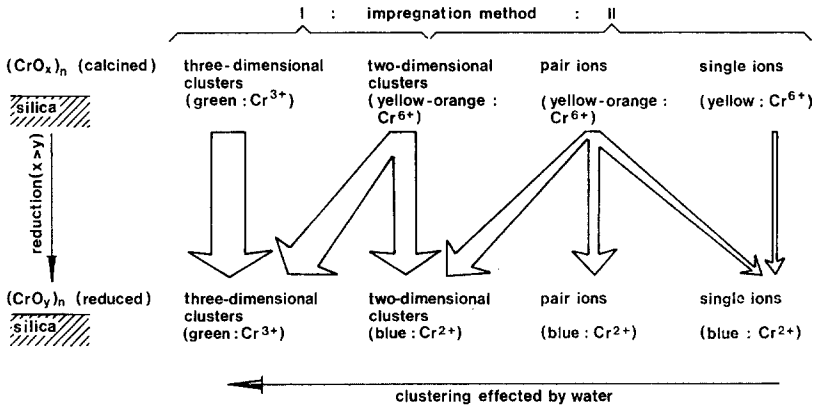

FIG. 12. The situation of chromium oxide on the silica surface after the calcination and the ensuing reduction considering different impregnation methods.

α-Cr_2O_3) during the reduction. Cornet and Burwell (*33*) noticed similar hydrolysis effects with the system $Cr(acac)_3$ on silica.

In view of the foregoing the stabilization of the catalyst by cycling can stand for nothing else but the continual formation of more of the larger chromium oxide conglomerates (α-Cr_2O_3?) and saturation of the surface with water. Since in all cases the Curie–Weiss law was obeyed and no Néel point could be detected, it can be concluded that the conglomerates were never very large.

CONCLUSIONS

Considering the different impregnation methods the situation of chromium oxide on the silica after calcination and ensuing reduction can be described with the help of Fig. 12. With impregnation method I the two- and three-dimensional clusters are favored. Dependent on the size of the three-dimensional clusters the color of the catalyst after calcination remains yellow–orange, similar to two-dimensional clusters, or changes into green (decomposition of CrO_3 into Cr_2O_3), since the stabilization of CrO_3 by the silica surface decreases with an increasing chromium oxide particle size. With impregnation method II the chromium pairs and the two-dimensional clusters dominate. Next to the impregnation method the presence of water during the reduction promotes the formation of clusters, especially if a large amount of water is evolved as is the case for reduction with hydrogen.

During the CO reduction no water is produced, so only the water already present at the silica surface as hydroxyl groups will play a role. This amount of water is relatively small and it will promote the formation of clusters only to a small extent. However, these hydroxyl groups are very important in determining the degree of reduction of the catalyst, because of their ability to oxidize Cr^{2+} ions to Cr^{3+} ions. Combined with the fact that the three-dimensional chromium oxide conglomerates cannot be reduced further than Cr_2O_3 we believe that on going from catalyst (II; CO) via catalyst (II; H_2) to catalyst (I; H_2) there are more and maybe larger clusters and the catalyst is on the average less reduced.

ACKNOWLEDGMENTS

The authors wish to thank Mr. W. van Herpen for his technical assistance and for preparing the figures. One of us (C.G.) wishes to thank the Netherlands Organization for the Advancement of Pure Research (Z.W.O.) for financial aid during his investigations which have been carried out under the auspices of the Netherlands Foundation for Chemical Research (S.O.N.).

REFERENCES

1. Hogan, J. P., and Banks, R. L., BE 530.617 (24-1-1955) and U.S. 2.825.721 (to Phillips Petroleum Company).
2. Kearby, K. K., *in* "Catalysis" (P. H. Emmett, ed.), Vol. 3, p. 453. Reinhold, New York, 1955.
3. Dutch Normalization Institute, Standards for chemical analysis, NEN 3104 Cr. 1 (1964) and NEN 3104 Cr (VI). 1 (1965).
4. Koningsberger, D. C., Mulder, G. J., and Pelupessy, B., *J. Phys. E. Scient. Instr.* **6**, 306 (1973).
5. Poole, C. P., Jr., and MacIver, D. S., *Adv. Catal.* **17**, 223 (1967).
6. van Reijen, L. L., and Cossee, P., *Disc. Faraday Soc.* **41**, 277 (1966).
7. Groeneveld, C., Wittgen, P. P. M. M., Swinnen, H. P. M., Wernsen, A., and Schuit, G. C. A., *J. Catal.*, in press.
8. Moeseler, R., Horvath, B., Lindenau, D., Horvath, E. G., and Krauss, H. L., *Z. Naturforsch.* **31b**, 892 (1976).
9. "Gmelin's Handbuch der Anorganische Chemie," p. 9. Chrom Teil B. Verlag Chemie GmbH, Weinheim, 1962.
10. Matsunaga, J., *Bull. Chem. Soc. Japan* **30**, 868, 984 (1957).
11. Holm, V. C. F., and Clark, A. J.. *J. Catal.* **11**, 305 (1968).
12. Hogan J. P., *J. Polym. Sci. A-1* **8**, 2637 (1970).
13. Ballhausen, C. J., "Introduction to Ligand Field Theory," p. 235. McGraw-Hill, New York, 1962.
14. Krauss, H. L., and Stach, H., *Z. Anorg. Allg. Chem.* **366**, 34 (1969).
15. van Reijen, L. L., Thesis, Eindhoven University of Technology (1964).
16. Kazanski, V. B., *Kinet. Catal.* **8**, 960 (1967).
17. Kazanski, V. B., and Turkevich, J., *J. Catal.* **8**, 231 (1967).
18. Al't, L. Ya., Anufrienko, V. F., Tyulikova, T. Ya., and Ermakov, Yu. I., *Kinet. Catal.* **9**, 1031 (1968).
19. Carman, C. J., and Kroenke, W. J., *J. Phys. Chem.* **72**, 2562 (1968).
20. Karapet'yants, M. Kh., and Karapet'yants, M. L., "Thermodynamic Constants of Inorganic and Organic Compounds," p. 74. Humphrey Science Publishers, London, 1970.
21. Benesi, H. A., and Jones, A. C., *J. Phys. Chem.* **63**, 179 (1959).
22. van Reijen, L. L., Sachtler, W. M. H., Cossee, P., and Brouwer, D. M., Proc. 3rd Intern. Congr. Catal. (Amsterdam 1964), p. 829. North-Holland, Amsterdam, 1965.
23. Carrà, S., and Forni, L., *Catal. Rev.* **5**, 159 (1971).
24. Kittel, C. H., "Introduction to Solid State Physics," 3rd ed. John Wiley, New York, 1968.
25. Eischens, R. P., and Selwood, P. W., *J. Amer. Chem. Soc.* **69**, 1590 (1947).
26. Srivastava, K. G., *Compt. Rend.* **253**, 2887 (1961).
27. Krauss, H. L., Rebenstorf, B., and Westphal, U., *Z. Anorg. Allg. Chem.* **414**, 97 (1975).
28. Freude, D., Oehme, W., Schmiedel, H. and Staudte, B., *J. Catal.* **32**, 137 (1974).
29. Wittgen, P. P. M. M., Groeneveld, C., Janssens, J. H. G. J., Wetzels, M. L. J. A., and Schuit, G. C. A., *J. Catal.* **59**, 168 (1979).
30. Wittgen, P. P. M. M., Groeneveld, C., Zwaans, P. J. C. J. M., Morgenstern, H. J. B., van Heugten, A. H., van Heumen, C. J. M., and Schuit, G. C. A., *J. Catal.*, in press.
31. Schuit, G. C. A., and de Boer, N. H., *Rec. Trav. Chim.* **70**, 1067 (1951).
32. Groeneveld, C., Wittgen, P. P. M. M., Lavrijsen, J. P. M., and Schuit, G. C. A., *J. Catal.*, in press.
33. Cornet, D., and Burwell, R. L. Jr., *J. Amer. Chem. Soc.* **90**, 2489 (1968).